

Conformationally Locked Chromophores as Models of Excited-State Proton Transfer in Fluorescent Proteins

Mikhail S. Baranov,[†] Konstantin A. Lukyanov,[†] Alexandra O. Borissova,[‡] Jordan Shamir,^{§,⊥} Dmytro Kosenkov,^{||} Lyudmila V. Slipchenko,^{||} Laren M. Tolbert,[§] Ilia V. Yampolsky,^{*,†} and Kyril M. Solntsev^{*,§}

[†]Institute of Bioorganic Chemistry, Russian Academy of Sciences, Miklukho-Maklaya 16/10, 117997 Moscow, Russia

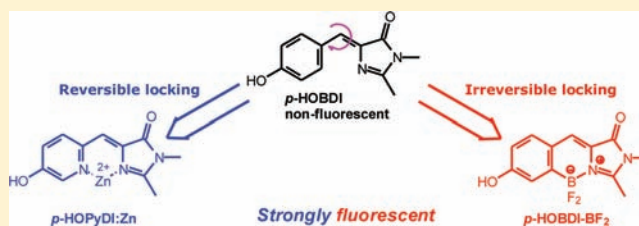
[‡]Nesmeyanov Institute of Organoelement Compounds, Russian Academy of Sciences, Vavilova 28, 119991 Moscow, Russia

[§]School of Chemistry and Biochemistry, Georgia Institute of Technology, 901 Atlantic Drive, Atlanta, Georgia 30332-0400, United States

^{||}Department of Chemistry, Purdue University, 560 Oval Drive, West Lafayette, Indiana 47907-2084, United States

Supporting Information

ABSTRACT: Members of the green fluorescent protein (GFP) family form chromophores by modifications of three internal amino acid residues. Previously, many key characteristics of chromophores were studied using model compounds. However, no studies of intermolecular excited-state proton transfer (ESPT) with GFP-like synthetic chromophores have been performed because they either are nonfluorescent or lack an ionizable OH group. In this paper we report the synthesis and photochemical study of two highly fluorescent GFP chromophore analogues: *p*-HOBDI-BF₂ and *p*-HOPyDI:Zn. Among known fluorescent compounds, *p*-HOBDI-BF₂ is the closest analogue of the native GFP chromophore. These irreversibly (*p*-HOBDI-BF₂) and reversibly (*p*-HOPyDI:Zn) locked compounds are the first examples of fully planar GFP chromophores, in which photoisomerization-induced deactivation is suppressed and protolytic photodissociation is observed. The photophysical behavior of *p*-HOBDI-BF₂ and *p*-HOPyDI:Zn (excited state pK_a's, solvatochromism, kinetics, and thermodynamics of proton transfer) reveals their high photoacidity, which makes them good models of intermolecular ESPT in fluorescent proteins. Moreover, *p*-HOPyDI:Zn is a first example of "super" photoacidity in metal–organic complexes.



INTRODUCTION¹

Members of the green fluorescent protein (GFP) family are now extensively used in experimental biology as genetically encoded fluorescent markers.² In contrast to other natural pigments whose biosyntheses involve multiple enzymes and cofactors, GFP-like proteins form chromophore groups by modifications of three internal amino acid residues. These modifications are fully catalyzed by the fluorescent protein (FP) itself and require no external enzymatic activities and cofactors except for molecular oxygen. The unique capability of unassisted chromophore formation is based on the spatial structure of fluorescent proteins. All GFP-like proteins share the same fold, which includes an 11-sheet β -barrel with a distorted α -helix inside the barrel. A chromophore is formed on this helix by cyclization and oxidation of the protein backbone at positions 65–67 (e.g., Ser65-Tyr66-Gly67 in GFP from jellyfish *Aequorea victoria*; here and below the numbering is in accordance with *A. victoria* GFP) and is located in the geometrical center of the β -barrel. Buried residues surrounding the chromophore (mainly those located in the middle of the β -strands) catalyze chromophore formation and participate in fine-tuning of its spectral properties.

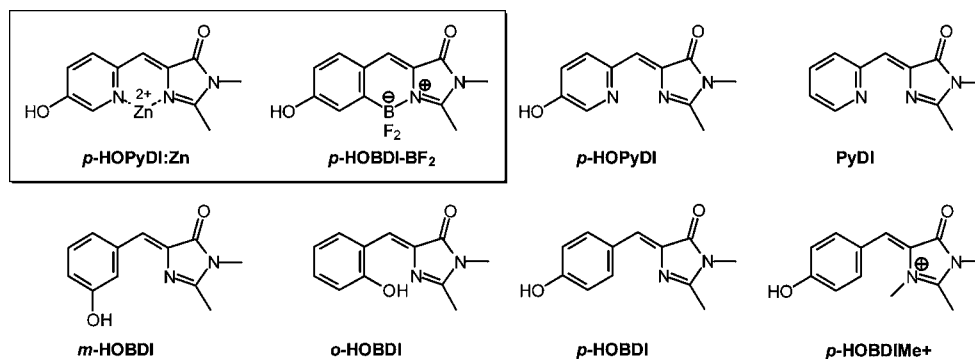
The chromophore in GFP is a 5-(4-hydroxybenzylidene)-3,5-dihydro-4*H*-imidazol-4-one.³ This bicyclic structure originates from the six-membered aromatic ring of the Tyr66 and a five-membered heterocycle formed by condensation of the carbonyl carbon of a residue at position 65 with the nitrogen of Gly67. It was found that Tyr66 can be mutated to aromatic residues with formation of blue-shifted chromophores.⁴ In particular, cyan and blue mutants of *A. victoria* GFP carry Trp66 and His66, respectively. The most blue-shifted spectra were achieved in the Phe66-containing protein Sirius with excitation at 355 and emission at 424 nm.⁵ Further chemical modifications of residue 65 of the core green chromophore can occur in natural GFP-like proteins.² These modifications extend a system of conjugated double bonds and result in strongly red-shifted spectra in yellow, orange, and red FPs and purple-blue chromoproteins.

Importantly, ionization of the phenolic hydroxyl of chromophore Tyr66 changes the spectra dramatically. FPs with a protonated (neutral) green chromophore possess an

Received: January 31, 2012

Published: March 8, 2012

Chart 1. Locked (in the Box) and Unlocked GFP Chromophores Discussed in the Text



absorption peak at about 400 nm, while chromophore deprotonation leads to an 80–90 nm absorption red shift. A similar dependence is observed for red FPs: they absorb at about 450 and 550–600 nm with protonated and deprotonated chromophores, respectively. Protonated chromophores can produce a corresponding short-wavelength emission (blue for green FPs or green for red FPs), but more typically they undergo ultrafast excited-state proton transfer (ESPT) and emit at longer wavelengths, similar to emission of the corresponding anionic chromophore.⁶ Perhaps the most studied example of ESPT in GFP-like proteins is the *A. victoria* wild-type (wt) GFP. The absorption spectrum of this protein possesses a major peak at 398 nm (protonated chromophore) and a minor peak at 478 nm (deprotonated chromophore).⁷ Notably, due to efficient ESPT, excitation of the wtGFP at either peak produces green fluorescence with only slightly different maxima (508 and 503 nm for excitation at 398 and 482 nm, respectively). Time-resolved spectroscopy demonstrates that excitation at 398 nm gives off a short-lived blue emission at about 460 nm which converts into green emission on a picosecond time scale.^{6a} A pathway of proton migration within the GFP β -barrel which includes a water molecule, Ser205, and Glu222 has been proposed.⁸ According to an alternative model, a proton from the excited chromophore can exit to the protein surface via Thr203, while reprotonation of the chromophore can occur due to a long proton entry pathway starting from Glu5 at the protein surface and continuing with several inner water molecules and residues including Glu222 and Ser205.⁹

The chemical and physical principles of chromophore formation and functioning in GFP-like proteins have generated keen interest. A number of different approaches, including crystallography, biochemical studies of native and hydrolyzed fluorescent proteins, directed and random mutagenesis, and steady-state and time-resolved spectroscopy, have been applied to study these issues.^{2–9} Among others, chemical synthesis of model chromophores was found to be a useful approach to confirm or refute structures suggested from structural studies, as well as to clarify details of chemical and spectral behavior of fluorescent proteins' chromophores.¹⁰ Our groups have developed and studied extended libraries of the GFP and RFP synthetic chromophores.¹¹ The simplest compound identical to the native GFP core is 4-(4-hydroxybenzylidene)-1,2-dimethyl-1*H*-imidazol-5(4*H*)-one (*p*-HOBDI, Chart 1). The fluorescence properties of this model chromophore differ dramatically from those of the wtGFP. Due to the very efficient photoisomerization-induced deactivation, its fluorescence quantum yield (FQY) is $<10^{-4}$, and the fluorescence lifetime in most solvents is <1 ps.¹² As a result, no intermolecular ESPT

has ever been observed in *p*-HOBDI in all solvents studied. Other model chromophores carry various substituents on this core or represent a modified artificial core similar, but not identical, to the chromophores in native fluorescent proteins. Using model compounds, many key characteristics of chromophores have been studied, including spectral properties of charged and neutral (protonated/deprotonated) states of chromophores, the influence of solvents and various substituents on the chromophore spectra,¹³ the dependence of FQY on steric hindrance,^{13b,14} and the formation of mature chromophores from biomimetic precursors.¹⁵ At the same time, no studies of ESPT with GFP-like synthetic chromophores have been performed to date, because they either are nonfluorescent^{13b} or lack an ionizable (–OH) group.^{14a}

The Georgia Tech team has studied intermolecular ESPT in various protonation states of *m*-HOBDI.¹⁶ Depending on pH of the solution, photoinduced deprotonation of the hydroxyl group and protonation of the imidazolone were observed. The characteristic times of this process were in the range of several picoseconds. However, most of the ESPT steps were diabatic and did not lead to fluorescent products.

A study of *intramolecular* proton transfer in *o*-HOBDI has been published recently.¹⁷ However, such intramolecular ESPT results in strongly different spectral characteristics compared to those of *p*-HOBDI and wtGFP.

Here we report the synthesis and examine the photophysical behavior (including intermolecular ESPT) of two highly fluorescent GFP chromophore analogues. The first compound is “irreversibly locked” *p*-HOBDI analogue, locked by a BF₂ group ((*SZ*)-5-[(2-difluoroboryl-4-hydroxyphenyl)methylidene]-2,3-dimethyl-3,5-dihydro-4*H*-imidazol-4-one, *p*-HOBDI-BF₂, Chart 1), similar to the strategy of Burgess.^{14a} Among known fluorescent compounds, *p*-HOBDI-BF₂ is closest to the native GFP chromophore. The second is a hydroxy derivative (*p*-HOPyDI) of the fluorophore PyDI ([(*Z*)-1,2-dimethyl-4-(pyridin-2-ylmethylene)]-1*H*-imidazol-5(4*H*)-one, Chart 1) studied recently by the Georgia Tech group.^{14c} PyDI becomes fluorescent upon complexation with Zn²⁺ or Cd²⁺, therefore introducing a “reversible locking” strategy. Upon metal binding, no new emission bands (MLCT, etc.) were observed, confirming the absence of photoinduced electron transfer between the d¹⁰ Zn²⁺ ion and the PyDI ligand. Here we demonstrate the enhanced photoacidity of the *p*-HOPyDI:Zn metal complex.

RESULTS

Synthesis and Characterization of GFP Synthetic Chromophores.

An elegant borylation of aromatic com-

pounds with boron tribromide, directed by a neighboring nitrogen atom, was recently described.¹⁸ We have modified this method by using a “nonbasic base”—molecular sieves—instead of *N,N*-diisopropylethylamine (DIPEA) as HBr scavenger to introduce a bridging BF₂ group into the bicyclic structure of *p*-HOBDI. *p*-HOBDI was silyl-protected at phenol and then reacted with BBr₃ and finally worked up with tetrabutylammonium fluoride (TBAF), killing two birds with one stone: removing the protecting group and converting the dibromoboryl fragment into the more stable difluoroboryl analogue (Figure 1). Full synthetic procedures and characterization of *p*-HOBDI-BF₂ are presented in the Supporting Information.

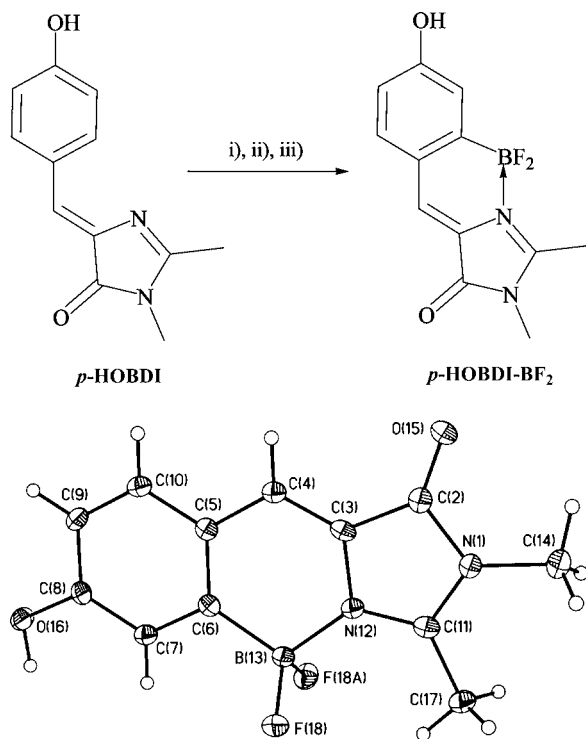


Figure 1. (Top) Synthesis of *p*-HOBDI-BF₂: (i) TBDPSCI, imidazole, DIPEA, THF; (ii) BBr₃, MS 4 Å, DCM; (iii) TBAF·EtOAc. (Bottom) General view of *p*-HOBDI-BF₂ with atoms represented as thermal ellipsoids at 50% probability level.

Crystals of *p*-HOBDI-BF₂ (C₁₂H₁₀BF₂N₂O₂, *M* = 263.03) grown from MeCN were light yellow, orthorhombic, space group *Pnma*. X-ray diffraction data were collected using a Bruker SMART APEX2 CCD diffractometer ($\lambda(\text{Mo K}\alpha) = 0.71073$ Å, graphite monochromator) at 100(2) K: *a* = 17.743(5), *b* = 6.6328(17), and *c* = 9.856(3) Å. Intensities of 11 350 reflections were measured, and 1378 independent reflections ($R_{\text{int}} = 0.0757$) were used in further refinement. Initially spherical atom refinements were undertaken with SHELXTL PLUS 5.0,¹⁰ using the full-matrix least-squares method. All non-hydrogen atoms were allowed to have an anisotropic thermal motion. The refinement converged to $wR2 = 0.0977$ and $\text{GOF} = 1.000$ for all independent reflections ($R1 = 0.0397$ was calculated against *F* for 928 observed reflections with $I > 2\sigma(I)$). Atomic coordinates, bond lengths, bond angles, and thermal parameters have been deposited at the Cambridge Crystallographic Data Center (CCDC) with number 829645.

The crystallographic data confirm the desired structure of the locked chromophore (Figure 1). The molecule is strictly

planar: all the atoms except fluorine and the hydrogen atoms of the methyl groups occupy special positions on the mirror plane. A certain degree of delocalization manifests in C–C bond lengths; e.g., C(4)–C(5) and C(3)–C(4) bond lengths (1.439(3) and 1.355(3) Å, respectively) deviate from both classical single bond (1.48 Å) and double bond (1.34 Å) distances. *p*-HOBDI-BF₂ molecules in the crystal are linked in chains by relatively strong O(16)–H(16)⋯O(15) hydrogen bonds (O⋯O distance is 2.693(3) Å, O–H⋯O angle is 175°). In turn, these chains are organized in stacks by strong π -stacking interactions with π ⋯ π distance ca. 3.3 Å. The parallel orientation of planar moieties is extremely favorable for strong stacking interactions. Stacks are linked by C–H⋯F interactions to form a 3D network.

p-HOPyDI was recently synthesized and characterized by Baldrige et al. as described in ref 19.

Steady-State and Time-Resolved Prototropic Behavior of *p*-HOBDI-BF₂. The absorption and emission spectra of *p*-HOBDI-BF₂ in various solvents resembled those of *p*-HOBDI but exhibited a 30–40 nm bathochromic shift (see Table S1). Indeed, only the neutral and anionic forms of the chromophores can be compared since the cationic form of *p*-HOBDI-BF₂ cannot be produced. However, the most important difference was the dramatic fluorescence turn-on of the locked *p*-HOBDI-BF₂. Its FQY in acetonitrile was 0.73, and the fluorescence lifetime in the absence of ESPT (τ_0) was 3.2 ns! This amazingly high value of FQY is close to those of wtGFP (0.79) and another boron-locked compound reported by Wu and Burgess (0.81).^{14a}

We²⁰ and others²¹ have successfully used the Kamlet–Taft multivariate approach²² for various hydroxyaromatic compounds, including *p*-HOBDI.²³ This approach correlates the spectral shift ν of the solute with the solvent parameters that are responsible for its acidic (α), basic (β), and polar solvating (π^*) properties.

$$\nu(1/\text{cm}) = \nu_0 + p\pi^* + a\alpha + b\beta \quad (1)$$

It allows a straightforward separation of selective (H-bonding) and nonselective (dipole–dipole interaction) solvation. We reported that the solvatochromic behavior of *p*-HOBDI and its derivatives upon absorption is governed by *both* polar and acid/base properties of the solvents. The magnitude of the *solute* parameters *p* can be related to the relative dipole moments of the molecules, while proton susceptibility parameters *a* and *b* reflect relative proton basicity and acidity of the chromophore. The magnitudes and directions of the solvatochromic shifts strongly depended on the protonation state of the solute. Our analysis clearly demonstrated the increase of the dipole moment of *p*-HOBDI upon ionization and showed its amphoteric behavior. In this work, an exceptionally strong fluorescence of *p*-HOBDI-BF₂ allowed solvatochromic analysis of both absorption and emission spectra. As in *p*-HOBDI, the absorption of the neutral form of *p*-HOBDI-BF₂ has a weak solvent dependence, but the Kamlet–Taft linear regression analysis was unsatisfactory, with the correlation coefficient <0.5. In contrast, such analysis resulted in good to very good fits for the anion absorption and all emission data (Table 1)

The spectral shift of the anionic absorption was governed solely by the acidity of the solvent. It is interesting that the magnitude of this interaction decreased 2-fold in the excited state, showing the weakening of the anion basicity (or the

Table 1. Solvatochromic Parameters (in $10^3/\text{cm}$) Used in Multivariable Regression Fits of Absorption and Emission Data for Neutral and Anionic Forms of *p*-HOBDI-BF₂ and *p*-HOBDI (Anion abs Only) According to Eq 1

band	ν_0	p	a	b	R^a
anion abs	18.7	-0.1	1.5	0	0.95
<i>p</i> -HOBDI ^b	22.9	-1.4	1.7	0.53	0.94
neutral fluor	22.1	-1.1	-0.2	-0.5	0.83
anion fluor	18.4	-0.2	0.7	0	0.86

^aCorrelation coefficient. ^bMeasured in MeOH/H₂O 1/1 v/v. From ref 23.

increase of the neutral acidity) upon excitation. The same effect was observed by us for a number of photoacids.²⁰

In contrast to *p*-HOBDI, *p*-HOBDI-BF₂ was readily soluble in water. Absorption maxima of *p*-HOBDI-BF₂ in neutral and basic water exhibited bathochromic shifts as compared to those of *p*-HOBDI and were much closer to the absorption maxima of *p*-HOBDIME⁺ at the same conditions. As expected, upon an increase in pH the peak at 400 nm decreased, while the new peak at 485 nm increased (Figure 2a). These bands interconverted with an isosbestic point at 425 nm and a pK_a of 6.4.

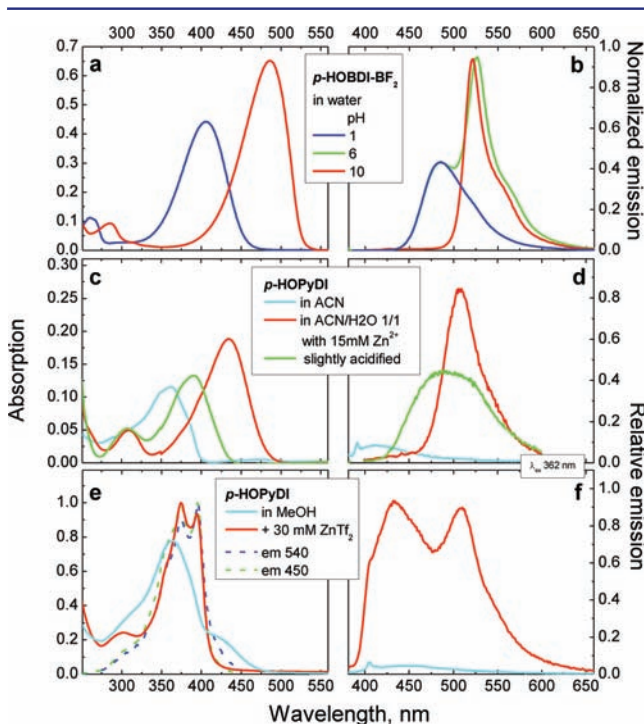


Figure 2. Absorption and emission of *p*-HOBDI-BF₂ and *p*-HOPyDI in various solvents. Absorbance spectra of *p*-HOBDI-BF₂ in water at pH 1 and 6 are identical.

In both protonated (R*OH) and deprotonated (R*O⁻) states, *p*-HOBDI-BF₂ fluoresced brightly. Excitation of the neutral absorption peak at 400 nm resulted in dual emission at 485 and 527 nm (Figure 2b). This phenomenon is a well-known intermolecular ESPT to water.²⁴ Our data are the first observation of the pronounced adiabatic ESPT in the GFP chromophore analogue, so we studied this reaction in detail. We found that interconversion of the blue and green emission peaks occurred at low pH with $pK_a^* = 2.1$ ²⁵ (Figure 3).

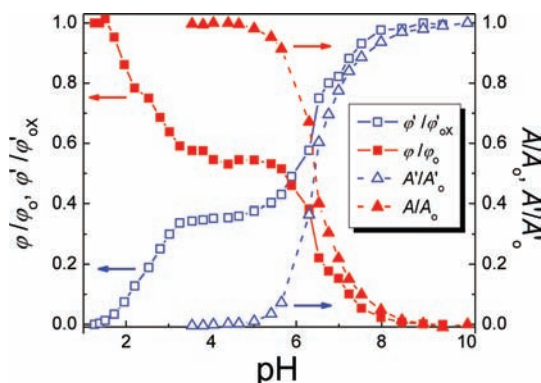


Figure 3. Fluorescence and absorption pH titration curves of *p*-HOBDI-BF₂ in water. ϕ/ϕ_0 (A/A_0) and ϕ'/ϕ'_{ox} (A'/A'_0) are the normalized fluorescence (absorption) intensities of R*OH (ROH) and R*O⁻ (RO⁻). Note that the intensity of R*O⁻ (ϕ'_{ox}) measured at the end of the titration curves is not the “real” one, since hydrolysis of *p*-HOBDI-BF₂ is observed. See Figure S3.

Utilization of the modified Förster cycle equation²⁵ resulted in $pK_a^* = 0.6$. Such moderate discrepancy between these methods is a common situation in the photoacid prototropic analysis and is usually associated with the errors in the spectral 0–0 energy transitions, as well as the presence of diabatic processes. Therefore, for the first time, we experimentally determined an excited-state pK_a of a close analogue of GFP chromophore.

Analysis of the fluorescence decay curves of R*OH and R*O⁻ in water resulted in an apparent dissociation rate constant $k_{ESPT} = 0.45$ 1/ns.²⁵ In the past, one of us²⁶ has analyzed the relationship between the kinetics and the thermodynamics of proton transfer from various hydroxyaromatic compounds in both the ground and excited states. All data were fitted by the unified Brønsted-type equation (Figure 4). In the current work we did not analyze this dependence but

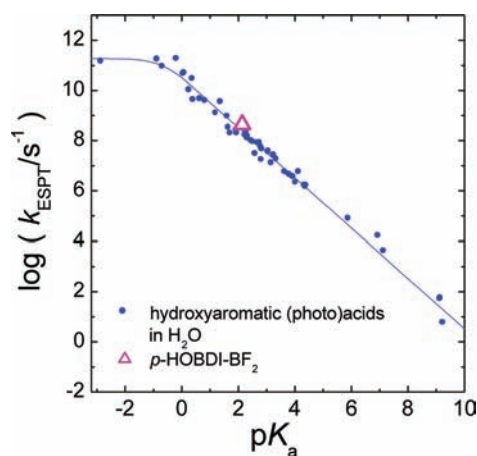


Figure 4. Relationship between the protolytic dissociation rate constants of various hydroxyaromatic compounds and their pK_a in water (Brønsted plot). Both ground- and excited-state proton transfer data are presented. Solid line is a fitting curve described in ref 26.

used it as a guideline. The ESPT data for *p*-HOBDI-BF₂ fit this plot perfectly, and this locked GFP chromophore falls into the range of moderate strength photoacids.

The excited-state behavior of *p*-HOBDI-BF₂ as a well-behaved moderate photoacid was further investigated by ESPT studies in methanol/water mixtures and by reaction with an

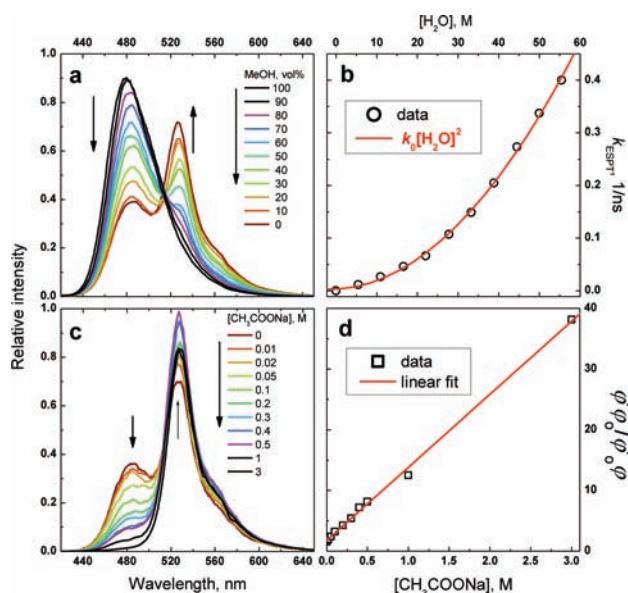


Figure 5. Effect of proton acceptor on the ESPT kinetics of *p*-HOBDBI-BF₂. Fluorescence spectra of *p*-HOBDBI-BF₂ in methanol/water mixtures (a) and in water at various concentrations of sodium acetate (c). Quadratic dependence of the ESPT rate constant MeOH/H₂O on [H₂O] (b). Stern–Volmer dependence (d).

external base. There is no ESPT from *p*-HOBDBI-BF₂ in pure methanol, as predicted for the photoacids with $pK_a^* > 0$.²⁷ Upon addition of water, the ESPT product band appeared in the emission spectra (Figure 5a). The ESPT rate constant had a quadratic dependence on water concentration (Figure 5b), as observed earlier for the photoacids with $pK_a^* > 0$.²⁸ Addition of an external base (acetate ion) to the aqueous solution of *p*-HOBDBI-BF₂ accelerated the observed ESPT (Figure 5c).²⁴ Analysis of the emission data using the modified Stern–Volmer equation (Figure 5d) resulted in the apparent bimolecular rate $3.8 \text{ M}^{-1} \text{ ns}^{-1}$. This diffusion-limited exergonic proton transfer from the excited GFP chromophore to the carboxylate does proceed on the ultrafast time scale in proteins, where the diffusion of the reagents is absent and the short proton wire supports a concerted proton transfer. It is interesting to draw parallels between the fluorescence spectrum of *p*-HOBDBI-BF₂ in 3 M sodium acetate solution and that of the H148D/S65T mutant²⁹ of the wtGFP. In both cases only the R^{*}O[−] emission is observed. Therefore, a 3 M concentration of proton acceptor in solution may mimic the chromophore–Asp interaction in H148D/S65T derived from the X-ray analysis.

Steady-State and Time-Resolved Prototropic Behavior of *p*-HOPyDI:Zn. Addition of the *para*-hydroxy group to the PyDI molecule resulted in the rich ground- and excited-state properties of *p*-HOPyDI. The latter molecule has five acid–base groups, but, to our surprise, the pH dependence of the absorption spectra resembled that of 3-hydroxypyridine.³⁰ This bifunctional compound exhibits a complicated pH dependence showing the equilibrium between the neutral, tautomeric (or zwitterionic), anionic, and cationic species. Similar prototropic behavior of *p*-HOBDBI indeed influences its ability to bind zinc ions and moderates the ground- and excited-state properties of the resulting complex.

First, we produced the Zn complex of *p*-HOPyDI using the method successfully utilized for PyDI:Zn synthesis.^{14c} Upon mixing of a very weakly fluorescent acetonitrile (or methanol) solution of *p*-HOPyDI with a 60 mM aqueous solution of zinc

nitrate, we observed a 73 nm bathochromic shift in the absorption spectrum (Figure 2c).²⁵ We attribute this band to the O-deprotonated state of the complex. At the same time, a moderate 10-fold fluorescence increase with a 62 nm bathochromic shift was observed in the emission spectrum (Figure 2d). Such modest fluorescence turn-on was much smaller than the 150-fold fluorescence increase in PyDI:Zn. We hypothesize that the moderate fluorescence turn-on in *p*-HOPyDI:Zn in aqueous solutions can be associated with the quenching by water. The latter may involve a non-adiabatic ESPT to water, as proposed by Manca³¹ for *p*-HOBDBI.

To exclude the possibility of quenching by water, and to check the occurrence of “super” photoacidity²⁷ in *p*-HOPyDI:Zn, we studied the formation and properties of this complex in nonaqueous media. The presence of 30 mM zinc triflate (ZnTf₂) in acetonitrile shifted the absorption band of the chromophore from 362 nm to the red-shifted band with vibronic maxima at 372 and 393 nm (Figure S4). The intensity of the single-band fluorescence of the *p*-HOPyDI:Zn complex in acetonitrile ($\lambda_{\text{max}} = 426 \text{ nm}$, $\phi = 0.029$, $\tau_0 = 145$ and 640 ps , amplitude ratio 7.8) was 120 times greater than that of a free ligand. We have not determined the structure of the complex, but by analogy with structurally similar PyDI:Zn^{14c} we assume that the stoichiometry of the *p*-HOPyDI:Zn complex is 1:1. Upon gradual addition of water, the vibronic structure in the absorption spectra became less pronounced, the emission of the 426 nm peak decreased, and the very weak emission band at 510 nm appeared due to the ground-state deprotonation and (to a minor extent) to ESPT to water (Figure S3). While the emission at 426 nm was quenched dramatically by water, the concomitant increase of the phenolate emission was negligible. This confirmed our hypothesis of the predominantly diabatic ESPT character in water.

Efficient formation of the highly fluorescent *p*-HOPyDI:Zn complex was also observed in dry methanol. Its absorption spectrum was similar to that of acetonitrile solution (Figures 2e and S4). However, in contrast to the latter, a pronounced two-band emission with maxima at 431 and 507 nm was observed in methanol (Figure 2f). Excitation spectra monitored at these bands were almost identical and perfectly matched the absorption spectrum (Figure 2e). This is evidence of efficient ESPT. To our knowledge, this is the first example of “super” photoacidity (i.e., ESPT to nonaqueous solvents)²⁷ of inorganic complexes. Similarly to acetonitrile/water mixtures, upon gradual addition of water to the methanol solution, the emission intensity of the R^{*}OH form decreased, while the emission of the anion practically did not change.

Keeping in mind that the complex may be unstable in aqueous solution, we diluted the methanol solution of *p*-HOPyDI:Zn with water up to 1/1 v/v and performed pH titration (Figure S5). The complex was stable only in a quite narrow pH range: $3.0 < \text{pH} < 6.2$. Nevertheless, the pK_a of the phenolic moiety can be estimated as 5.3 from both emission and absorption data. Using the Förster cycle equation (see above) and the emission/absorption maxima for the neutral (385/433 nm) and the anion (432/506 nm) of *p*-HOPyDI:Zn in methanol/water, we estimated the pK_a^* as -1.3 , confirming our classification of *p*-HOPyDI:Zn as a “super” photoacid.

The fluorescence lifetime of the *p*-HOPyDI:Zn neutral form in the presence of ESPT (τ) in methanol is 56 ps; its conjugated base has a rise time of 53 ps and decays with 110 ps lifetime. It is important to realize that the decay of the neutral form reflects the sum of adiabatic and diabatic ESPT.³² Because

of *p*-HOPyDI:Zn instability at the high or lower pH when the acid–base equilibrium is shifted to pure neutral or anionic, it is impossible to separate the rates of adiabatic and diabatic ESPT, so only the upper limit of the adiabatic k_{ESPT} can be determined.

Therefore, we have demonstrated the first example of the enormous photoacidity in an inorganic complex. This area is relatively undeveloped,³³ and usually the ΔpK_a between the ground and the excited states does not exceed 5 pK_a units.³⁴ It would be intriguing to synthesize complexes of *p*-HOPyDI with heavy metals such as Pt that would promote efficient intersystem crossing. The resulting long-lived triplet state may exhibit a dramatic photoacidity as well.²⁴ Similarly, we can propose that the metal-dependent “turn-on” of photoacidity may have mechanistic and diagnostic consequences.

Theoretical Computations of *p*-HOBDI-BF₂ and *p*-HOPyDI:Zn Ground- and Excited-State Acidity. A deeper understanding of the ground- and excited- state acidity of novel compounds could be achieved using high-level calculations. Theoretical computations of pK_a^* are generally very daunting. A simple scheme has been employed in this work, with a goal to provide qualitative insight into the origins of differences in the pK_a^* between *p*-HOBDI-BF₂ and *p*-HOPyDI:Zn. The pK_a of the ground state of an acid (AH) can be calculated using the Gibbs free energy of a dissociation reaction $\text{AH} \rightarrow \text{A}^- + \text{H}^+$ in a solvent: $pK_a = \Delta G_{\text{aq}}/\ln(10)RT$. The Gibbs free energy ΔG_{aq} of the reaction can be evaluated using the Born–Haber cycle³⁵ as a sum of the gas-phase electronic energy $\Delta E_{\text{g}}^{\text{AH} \rightarrow \text{A}^-}$, zero-point vibrational energy $\Delta \text{ZPE}_{\text{g}}^{\text{AH} \rightarrow \text{A}^-}$, Gibbs free energy $\Delta G_{\text{g},0 \rightarrow 298\text{K}}^{\text{AH} \rightarrow \text{A}^-}$ and solvation energy $\Delta G_{\text{solv}}^{\text{AH} \rightarrow \text{A}^-}$ differences between protonated (AH) and deprotonated (A[−]) species:

$$\Delta G_{\text{aq}} = \Delta E_{\text{g}}^{\text{AH} \rightarrow \text{A}^-} + \Delta \text{ZPE}_{\text{g}}^{\text{AH} \rightarrow \text{A}^-} + \Delta G_{\text{g},0 \rightarrow 298\text{K}}^{\text{AH} \rightarrow \text{A}^-} + \Delta E_{\text{solv}}^{\text{AH} \rightarrow \text{A}^-} + \Delta G_{\text{g}}^{\text{H}^+} + \Delta G_{\text{solv}}^{\text{H}^+} \quad (2)$$

where $\Delta G_{\text{g}}^{\text{H}^+} = -6.28$ kcal/mol is the standard Gibbs free energy of the proton in the gas phase and $\Delta G_{\text{solv}}^{\text{H}^+}$ is the solvation free energy of the proton, estimated theoretically as -262.23 kcal/mol.³⁶ Gas-phase geometry optimizations, ZPE, and Gibbs free energies were computed at the B3LYP/6-31G(*) level of theory. Gibbs free energies in an aqueous solvent were estimated using PBE0/6-31+G(*) and a polarizable continuum model (PCM).³⁷ The excited-state pK_a^* values were obtained using the Förster cycle equation as a sum of the ground-state pK_a and the excitation energy difference $\Delta E_{\text{ex,solv}}^{\text{AH} \rightarrow \text{A}^-}$ between protonated and deprotonated species in a solvent:

$$pK_a^* = pK_a + \Delta E_{\text{ex,solv}}^{\text{AH} \rightarrow \text{A}^-} / \ln(10)RT \quad (3)$$

The excitation energies in a solvent were computed using time-dependent density functional theory (TD-DFT) at the PBE0/6-31+G(*) level of theory and PCM. Results of these calculations are summarized in Table 2.

In agreement with experimental findings, the optimized structures of *p*-HOBDI-BF₂ and *p*-HOPyDI:Zn are planar both in the gas phase and in aqueous solvent. Substituents in the *meta*-position with respect to the hydroxyl group influence a charge distribution on hydroxyl oxygen, as well as the vibrational frequencies of the OH stretch mode (3713 cm^{−1}

Table 2. Comparison of *p*-HOBDI-BF₂ and *p*-HOPyDI:Zn Kinetic and Thermodynamics Data: Fluorescence Quantum Yields, ESPT Rate Constants, pK_a , and pK_a^*

	<i>p</i> -HOBDI-BF ₂	<i>p</i> -HOPyDI:Zn
Experimental Data		
FQY ^a	0.73	0.029
τ_{or} , ns ^a	3.2	<0.21>
τ , ns	1.45 ^b	0.056 ^c
k_{ESPT} , 1/ns ^d	0.45 ^b	<13 ^c
pK_a	6.4 ^b	5.3 ^e
pK_a^*	2.1 ^{b,f}	−1.3 ^{e,g}
Computational Results		
q_{OH} ^h , au	−0.63	−0.57
$\Delta E_{\text{ex,solv}}$, kcal/mol	−8.07	−8.32
pK_a ^{b,i}	5.62	2.59
pK_a^* ^{b,j}	−0.30	−3.52

^aIn ACN. ^bIn water. ^cIn MeOH. ^dDetermined as $k_{\text{ESPT}} = 1/\tau - 1/\tau_{\text{or}}$. ^eIn MeOH/H₂O 2/1 v/v. ^fFrom fluorescence pH titration. ^gFrom Förster equation. ^hThe Mulliken charges on hydroxyl oxygen in protonated species. ⁱFrom eq 2. ^jFrom eq 3.

in *p*-HOPyDI:Zn versus 3737 cm^{−1} in *p*-HOBDI-BF₂). This suggests that the positively charged Zn substitution weakens the OH bond strength and promotes deprotonation. The calculated ground-state pK_a values are in agreement with this qualitative analysis. The acidity of both compounds decreases by 5.9–6.1 units upon excitation, placing them as “super” photoacids. However, taking into account that the computed ground-state pK_a values are probably underestimated, there is a nice agreement between theory and experiment in both the relative acidity of *p*-HOPyDI:Zn and *p*-HOBDI-BF₂ and the increase of the acidity upon excitation.

CONCLUSIONS

We have demonstrated the first known examples of fully planar synthetic GFP chromophores, in which photoisomerization-induced deactivation is suppressed and efficient *intermolecular* ESPT is observed. A pronounced difference in the photoacidity of *p*-HOBDI-BF₂ and *p*-HOPyDI:Zn was established. Of course, we note that these compounds carry oppositely charged substituents in the position meta to the reactive hydroxyl group. Such meta-effects are known to influence the excited-state acidity dramatically.³⁸ We propose that the pK_a^* values of these compounds may serve as the lower and upper estimates for the pK_a^* of unsubstituted *p*-HOBDI. The theoretical pK_a^* of *p*-HOBDI (0.1 in water)³⁹ calculated by Scharnagl and Raupp-Kossmann fits nicely within these boundaries.

ASSOCIATED CONTENT

Supporting Information

Synthetic procedures, additional spectral data, and pH titration curves of *p*-HOBDI-BF₂. This material is available free of charge via the Internet at <http://pubs.acs.org>.

AUTHOR INFORMATION

Corresponding Author

ivyamp@gmail.com; solntsev@gatech.edu; <http://ww2.chemistry.gatech.edu/solntsev>

Notes

The authors declare no competing financial interest.

[†]Summer program participant (high school student) from Lawrenceville School, 2500 Main St., Lawrenceville, NJ 08648

ACKNOWLEDGMENTS

Financial support from the National Science Foundation (CHE-0809179 for K.M.S. and Career CHE-0955419 for L.V.S.) is gratefully acknowledged. We thank the Department of Energy, Office of Basic Science (DE-FG02-04ER46141), for generous financial support to L.M.T. L.V.S. acknowledges support from Purdue University. The Moscow group acknowledges grants by the Molecular and Cell Biology Program of the Russian Academy of Sciences, and Ministry of Education and Science of the Russian Federation (16.740.11.0367 and 16.512.11.2139). We thank Anthony Baldrige for providing *p*-HOPyDI, and Julia Weinstein for stimulating discussions.

REFERENCES

- (1) This is part of our series "Photochemistry of "super" photoacids". For the previous paper, see: Gould, E.-A.; Popov, A. V.; Tolbert, L. M.; Presiado, I.; Erez, Y.; Huppert, D.; Solntsev, K. M. *Phys. Chem. Chem. Phys.* **2012**, DOI: 10.1039/c2cp23891h.
- (2) Chudakov, D. M.; Matz, M. V.; Lukyanov, S.; Lukyanov, K. A. *Physiol. Rev.* **2010**, 1103.
- (3) Cody, C. W.; Prasher, D. C.; Westler, W. M.; Prendergast, F. G.; Ward, W. W. *Biochemistry* **1993**, 32, 1212.
- (4) Heim, R.; Prasher, D. C.; Tsien, R. Y. *Proc. Natl. Acad. Sci. U.S.A.* **1994**, 91, 12501.
- (5) Tomosugi, W.; Matsuda, T.; Tani, T.; Nemoto, T.; Kotera, I.; Saito, K.; Horikawa, K.; Nagai, T. *Nat. Methods* **2009**, 6, 351.
- (6) (a) Chatteraj, M.; King, B. A.; Bublitz, G. U.; Boxer, S. G. *Proc. Natl. Acad. Sci. U.S.A.* **1996**, 93, 8362. (b) Kogure, T.; Karasawa, S.; Araki, T.; Saito, K.; Kinjo, M.; Miyawaki, A. *Nat. Biotechnol.* **2006**, 24, 577. (c) Henderson, J. N.; Osborn, M. F.; Koon, N.; Gepshtein, R.; Huppert, D.; Remington, S. J. *J. Am. Chem. Soc.* **2009**, 131, 13212. (d) Piatkevich, K. D.; Malashkevich, V. N.; Almo, S. C.; Verkhusa, V. V. *J. Am. Chem. Soc.* **2010**, 132, 10762.
- (7) Ward, W. W.; Bokman, S. H. *Biochemistry* **1982**, 21, 4535.
- (8) (a) Palm, G. J.; Zdanov, A.; Gaitanaris, G. A.; Stauber, R.; Pavlakis, G. N.; Wlodawer, A. *Nat. Struct. Biol.* **1997**, 4, 361. (b) Brejc, K.; Sixma, T. K.; Kitts, P. A.; Kain, S. R.; Tsien, R. Y.; Ormö, M.; Remington, S. J. *Proc. Natl. Acad. Sci. U.S.A.* **1997**, 94, 2306.
- (9) Agmon, N. *Biophys. J.* **2005**, 88, 2452.
- (10) (a) Niwa, H.; Inouye, S.; Hirano, T.; Matsuno, T.; Kojima, S.; Kubota, M.; Ohashi, M.; Tsuji, F. I. *Proc. Natl. Acad. Sci. U.S.A.* **1996**, 93, 13617. (b) Bell, A. F.; He, X.; Wachter, R. M.; Tonge, P. T. *Biochemistry* **2000**, 39, 4423. (c) Voityuk, A. A.; Kummer, A. D.; Michel-Beyerle, M.-E.; Rösch, N. *Chem. Phys.* **2001**, 269, 83. (d) Yampolsky, I. V.; Remington, S. J.; Martynov, V. I.; Potapov, V. K.; Lukyanov, S.; Lukyanov, K. A. *Biochemistry* **2005**, 44, 5788.
- (11) (a) Ivashkin, P. E.; Yampolsky, I. V.; Lukyanov, K. A. *Russ. J. Bioorg. Chem.* **2009**, 35, 652. (b) Tolbert, L. M.; Baldrige, A.; Kowalik, J.; Solntsev, K. M. *Acc. Chem. Res.* **2012**, 45, 171.
- (12) Mandal, D.; Tahara, T.; Meech, S. R. *J. Phys. Chem. B* **2004**, 108, 1102.
- (13) (a) Kojima, S. *Tetrahedron Lett.* **1998**, 39, 5239. (b) Niwa, H.; Inouye, S.; Hirano, T.; Matsuno, T.; Kojima, S.; Kubota, M.; Ohashi, M.; Tsuji, F. I. *Proc. Natl. Acad. Sci. U.S.A.* **1996**, 93, 13617. (c) He, X.; Bell, A. F.; Tonge, P. J. *Org. Lett.* **2002**, 4, 1523. (d) Yampolsky, I. V.; Remington, S. J.; Martynov, V. I.; Potapov, V. K.; Lukyanov, S.; Lukyanov, K. A. *Biochemistry* **2005**, 44, 5788. (e) Yampolsky, I. V.; Kislukhin, A. A.; Amatov, T. T.; Shcherbo, D.; Potapov, V. K.; Lukyanov, S.; Lukyanov, K. A. *Bioorg. Chem.* **2008**, 36, 96. (f) Yampolsky, I. V.; Balashova, T. A.; Lukyanov, K. A. *Biochemistry* **2009**, 48, 8077.
- (14) (a) Wu, L.; Burgess, K. *J. Am. Chem. Soc.* **2008**, 130, 4089. (b) Conyard, J.; Kondo, M.; Heisler, I. A.; Jones, G.; Baldrige, A.; Tolbert, L. M.; Solntsev, K. M.; Meech, S. R. *J. Phys. Chem. B* **2011**, 115, 1571. (c) Baldrige, A.; Solntsev, K. M.; Song, C.; Tanioka, T.; Kowalik, J.; Hardcastle, K.; Tolbert, L. M. *Chem. Commun.* **2010**, 46, 5686.
- (15) (a) Kojima, S.; Hirano, T.; Niwa, H.; Ohashi, M.; Inouye, S.; Tsuji, F. I. *Tetrahedron Lett.* **1997**, 38, 2875. (b) Ivashkin, P. E.; Lukyanov, K. A.; Lukyanov, S.; Yampolsky, I. V. *J. Org. Chem.* **2011**, 76, 2782.
- (16) (a) Dong, J.; Solntsev, K. M.; Poizat, O.; Tolbert, L. M. *J. Am. Chem. Soc.* **2007**, 129, 10084. (b) Solntsev, K. M.; Poizat, O.; Dong, J.; Rehault, J.; Lou, Y.; Burda, C.; Tolbert, L. M. *J. Phys. Chem. B* **2008**, 112, 2700.
- (17) Hsieh, C.-C.; Chou, P.-T.; Shih, C.-W.; Chuang, W.-T.; Chung, M.-W.; Lee, J.; Joo, T. *J. Am. Chem. Soc.* **2011**, 133, 2932.
- (18) Ishida, N.; Moriya, T.; Goya, T.; Murakami, M. *J. Org. Chem.* **2010**, 75, 8709.
- (19) Lee, J.-S.; Baldrige, A.; Feng, S.; SiQiang, Y.; Kim, Y. K.; Tolbert, L. M.; Chang, Y.-T. *ACS Comb. Sci.* **2011**, 13, 32.
- (20) (a) Solntsev, K. M.; Huppert, D.; Tolbert, L. M.; Agmon, N. *J. Am. Chem. Soc.* **1998**, 120, 7981. (b) Solntsev, K. M.; Huppert, D.; Agmon, N. *J. Phys. Chem. A* **1998**, 102, 9599. (c) McGrier, P. L.; Solntsev, K. M.; Miao, S.; Tolbert, L. M.; Miranda, O. R.; Rotello, V. M.; Bunz, U. H. F. *Chem.—Eur. J.* **2008**, 14, 4503.
- (21) (a) Mijin, D. Ž.; Ušćumlić, G. S.; Perišić-Janjić, N. U.; Valentić, N. V. *Chem. Phys. Lett.* **2006**, 418, 223. (b) Reta, M.; Cattana, R.; Silber, J. J. *J. Solution Chem.* **2001**, 30, 237. (c) Magnes, B.-Z.; Pines, D.; Strashnikova, N.; Pines, E. *Solid State Ionics* **2004**, 168, 225. (d) Volkin, A. I.; Sherstyannikova, L. V.; Kanitskaya, L. V.; Abzaeva, K. A.; Lopyrev, V. A.; Turchaninov, V. K. *Russ. J. Gen. Chem.* **2001**, 71, 1708.
- (22) Kamlet, M. J.; Abboud, J. L. M.; Abraham, M. H.; Taft, R. W. *J. Org. Chem.* **1983**, 48, 2877.
- (23) Dong, J.; Solntsev, K. M.; Tolbert, L. M. *J. Am. Chem. Soc.* **2006**, 128, 12038.
- (24) (a) Yu, I.; Martynov, A. B.; Demyashkevich, B. M. U.; M. G., K. *Russ. Chem. Rev.* **1977**, 46, 1. (b) Weller, A. *Prog. React. Kinet.* **1961**, 1, 189. (c) Arnaut, L.; Formosinho, S. J. *J. Photochem. Photobiol. A* **1993**, 75, 1.
- (25) See Supporting Information for more details.
- (26) Solntsev, K. M.; Al-Ainain, S. A.; Il'ichev, Y. V.; Kuzmin, M. G. *J. Phys. Chem. A* **2004**, 108, 8212.
- (27) Tolbert, L. M.; Solntsev, K. M. *Acc. Chem. Res.* **2002**, 35, 19.
- (28) Solntsev, K. M.; Huppert, D.; Agmon, N.; Tolbert, L. M. *J. Phys. Chem. A* **2000**, 104, 4658.
- (29) (a) Leiderman, P.; Genosar, L.; Huppert, D.; Shu, X.; Remington, S. J.; Solntsev, K. M.; Tolbert, L. M. *Biochemistry* **2007**, 46, 12026. (b) Stoner-Ma, D.; Jaye, A. A.; Ronayne, K. L.; Nappa, J.; Meech, S. R.; Tonge, P. J. *J. Am. Chem. Soc.* **2008**, 130, 1227.
- (30) (a) Metzler, D. E.; Harris, C. M.; Johnson, R. J.; Siano, D. B.; Thomson, J. A. *Biochemistry* **1973**, 12, 5377. (b) Reiter, J.; Beyer, A.; Potschka, M.; Schuster, P.; Winkler, H.; Ebeling, H.; Franck, E. U. *J. Phys. Chem.* **1989**, 93, 442. (c) D'Angel, J. C.; Collette, T. W. *Anal. Chem.* **1997**, 69, 1642.
- (31) Manca, C. *Chem. Phys. Lett.* **2007**, 443, 173.
- (32) Solntsev, K. M.; Al-Ainain, S. A.; Il'ichev, Y. V.; Kuzmin, M. G. *J. Photochem. Photobiol. A* **2005**, 175, 178.
- (33) (a) Vos, J. G. *Polyhedron* **1992**, 11, 2285. (b) Liu, W.; Thorp, H. H. *Adv. Transition Met. Coord. Chem.* **1996**, 1, 187.
- (34) (a) Giordano, P. J.; Bock, C. R.; Wrighton, M. S. *J. Am. Chem. Soc.* **1978**, 100, 6960. (b) Cattaneo, M.; Fagalde, F.; Katz, N. E. *Inorg. Chem.* **2006**, 45, 6884. (c) Su, C.-H.; Chen, H.-Y.; Tsai, K. Y.-D.; Chang, I.-J. *J. Phys. Chem. B* **2007**, 111, 6857. (d) Han, M.-J.; Chen, Y.-M.; Wang, K.-Z. *New J. Chem.* **2008**, 32, 970.
- (35) (a) Jacquemin, D.; Perpète, E. A.; Ciofini, I.; Adamo, C. *J. Phys. Chem. A* **2008**, 112, 794. (b) Jang, Y. H.; Goddard, W. A. III; Noyes, K. T.; Sowers, L. C.; Hwang, S.; Chung, D. S. *J. Phys. Chem. B* **2003**, 107, 344.
- (36) Tawa, G. J.; Topol, I. A.; Burt, S. K.; Caldwell, R. A.; Rashin, A. A. *J. Chem. Phys.* **1998**, 109, 4852.
- (37) Tomasi, J.; Mennucci, B.; Cammi, R. *Chem. Rev.* **2005**, 105, 2999.
- (38) (a) Zimmerman, H. E. *J. Am. Chem. Soc.* **1995**, 117, 8988. (b) Lewis, F. D.; Yang, J.-S. *J. Am. Chem. Soc.* **1997**, 119, 3834.

(39) Scharnagl, C.; Raupp-Kossmann, R. A. *J. Phys. Chem. B* **2004**, *108*, 477.